IEEE Access
Multidisciplinary | Rapid Review | Open Access Journal

Received August 12, 2021, accepted August 25, 2021, date of publication August 30, 2021, date of current version September 8, 2021.

Digital Object Identifier 10.1109/ACCESS.2021.3109068

Analysis and Design of a Novel Outer Mover Moving Magnet Linear Oscillating Actuator for a Refrigeration System

ZAHOOR AHMAD[1], ADNAN HASSAN[2], (Member, IEEE), FAISAL KHAN[1], (Member, IEEE), NASEER AHMAD[3], BAKHTIAR KHAN[1], (Member, IEEE), AND JONG-SUK RO[4,5]

[1]Electrical and Computer Engineering Department, COMSATS University Islamabad at Abbottabad, Abbottabad, Khyber Pakhtunkhwa 22060, Pakistan
[2]Mechatronics Engineering Department, Istanbul Bilgi University, 34060 Istanbul, Turkey
[3]Faculty of Information and Communication Technology, Balochistan University of Information Technology, Engineering and Management Sciences (BUITEMS), Quetta 87300, Pakistan
[4]School of Electrical and Electronics Engineering, Chung-Ang University, Dongjak-gu, Seoul 06974, Republic of Korea
[5]Department of Intelligent Energy and Industry, Chung-Ang University, Dongjak-gu, Seoul 06974, Republic of Korea

Corresponding author: Jong-Suk Ro (jongsukro@gmail.com)

This research was supported by Basic Science Research Program through the National Research Foundation of Korea funded by the Ministry of Education(2016R1D1A1B01008058) and Human Resources Development (No.20204030200090) of the Korea Institute of Energy Technology Evaluation and Planning(KETEP) grant funded by the Korea government Ministry of Trade, Industry and Energy.

ABSTRACT This article presents linear oscillating actuator (LOA) which generates bidirectional linear thrust force. Design topology of the proposed LOA contains an outer mover and an inner stator design. Two axially magnetized and tubular-shaped permanent magnets (PMs) are mounted on the mover. Due to the higher magnetic flux density of axially magnetized PMs in a specific direction, it generates higher thrust force than radially magnetized PMs. The proposed LOA operates on single-phase alternating source. All the design specifications of the LOA are optimized through finite element method (FEM) and optimum values of the design parameters are obtained. Output parameters such as the stroke length and thrust force are analyzed for multiple magnitudes of the input parameters such as current using FEM. Additionally, other parameters like back emf, coil current and winding resistance are analyzed at resonance. Effect of motor constant is investigated toward both directions of the force, which shows identical replication. Output parameters of the LOA are compared with already designed topologies of the LOA for refrigeration system. Proposed LOA demonstrates promising improvements in terms of motor constant and thrust force compared to the volume of the LOA. Moreover, proposed LOA is comparatively convenient to fabricate as well.

INDEX TERMS FEM, linear compressor, moving magnet linear actuator, outer mover design topology.

I. INTRODUCTION

LOA provides controlled linear oscillatory motion (LOM) between two extreme positions. Displacement of the moving part of the LOA between two peak points is called stroke of the LOA [1]. Compared to conventional actuation method where LOM is generated by a special mechanism called crankshaft, LOA produces LOM without using any intermediate conversion mechanism. The main drawback of the conventional actuation method is more friction points due to additional numbers of mechanical parts. Furthermore, in the conventional method, thrust force is decomposed into radial and tangential components, resulting in low efficiency of the machine [2], [3]. LOA gives LOM of specific frequency that is equal to the frequency of single-phase input alternating supply [4]. Advantages of the LOA over conventional method are: adjustable stroke, high frequency oscillations, easily controllable, reduced number of mechanical parts and lower fabrication cost. Moreover, LOAs work on a resonance frequency that can be picked on the basis of mover mass and spring constant. At this frequency, moving part (mover) requires less amount of electromagnetic thrust force [5]. Stator, static part of the LOA yields, controlled electromagnetic field and mover adjusts its position to provide least

The associate editor coordinating the review of this manuscript and approving it for publication was Padmanabh Thakur.

reluctance path to magnetic flux. Due to adjustment of the mover position, linear oscillations are produce [6]. Based on the mover moving part of the LOA, there are three types of mover configurations: moving magnet, moving iron and moving coil. Moving magnet type or moving magnet along with iron core is more efficient than others because of their characteristically high thrust density and efficiency of the actuator. Moreover, moving magnet actuator has fast response which is suited to harsh environment and low moving mass [7]–[9]. Stator configuration also influences the performance of LOA to a great extent. Configuration which provides ease to the flow of magnetic flux enhances the performance of LOA [10]. Radial magnetized tubular magnets are made of numbers of unidirectional magnets that reduce the mechanical strength of the mover and assembly of the actuator becomes complex. Moreover, it is difficult to perfectly magnetize radial magnet compared to axial magnets [11]. The magnetization of radial magnets is not perfectly radial and generates magnetic flux in different directions [12]. A radial magnetized outer mover moving magnet actuators are studied in [13], [14]. Numerous topologies are used for the design of LOA and these can be replaced by tubular structure and it is the best option given the reasons of solid packaging and volumetric efficiency [6]. Additionally, tubular assembly has no end winding, high air gap flux density and high efficiency [15].

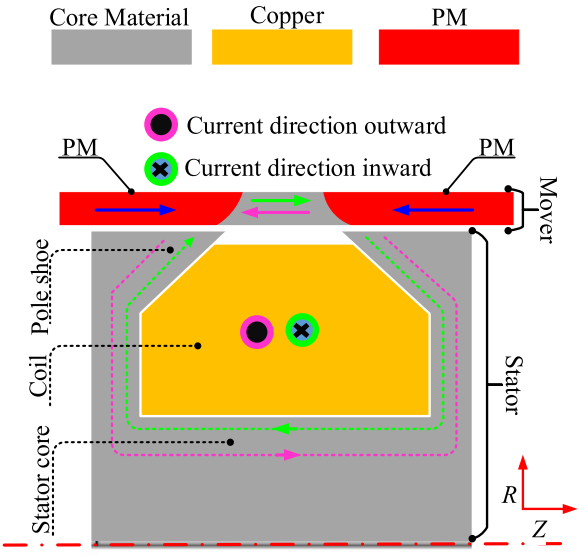

FIGURE 1. 2-D Axisymmetric topology of LOA.

Split ratio, the ratio of stator outer diameter to the stator inner diameter, is studied in [16]. This analysis concludes that optimal split ratio enhances the output parameter of the actuator like thrust force and efficiency. Consequence of the split ratio is variation in the mover mass. Mover mass causes an effect on the value of resonance frequency. Appropriate dimensions of the different parameters within constrained volume of LOA show significant effects on output parameter like thrust force and stroke [17]. Reduction

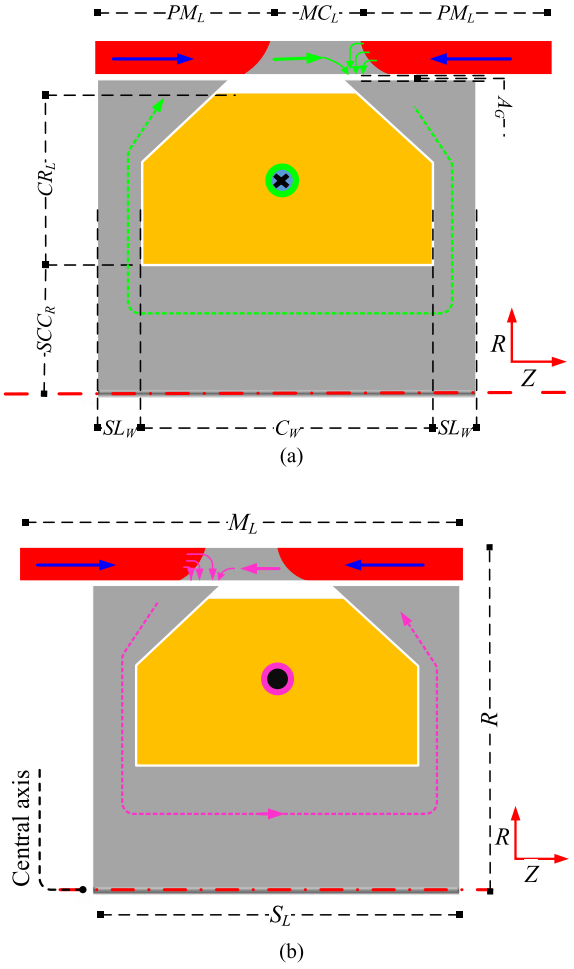

FIGURE 2. Bi-directional extreme positions of the mover (a) +z extreme position (b) −z extreme position.

of loses also improves the performance of the actuator. Different techniques are used for the reduction of iron loses. A method used in [18] is studied, which significantly reduces iron loses. Making the moving part of the electric motor slightly extended reduces the fringing effect that further improves the performance of LOA [19]. Some unwanted impact of mechanical bearing is affecting LOA. Mechanical bearings are replaced by a special levitation method in [20]. Since the main flaws using mechanical bearing are friction, uncleanness due to wear and lifetime. This approach proposes the concept of using magnetic bearings. Applications where small volume of actuator are required LOA is used due small size and high thrust density [21]. Proposed LOA can be used for several applications such as compressor for refrigeration system [1]–[6], robot, micro-positioning, and bio-medical machines [20], [22].

This paper proposes a novel topology of an outer mover moving magnet LOA using tubular shaped and axially magnetized PMs. 2-D axisymmetric structure and CAD model are used for better understanding of the structure and working principle of the LOA. Topology is optimized by using

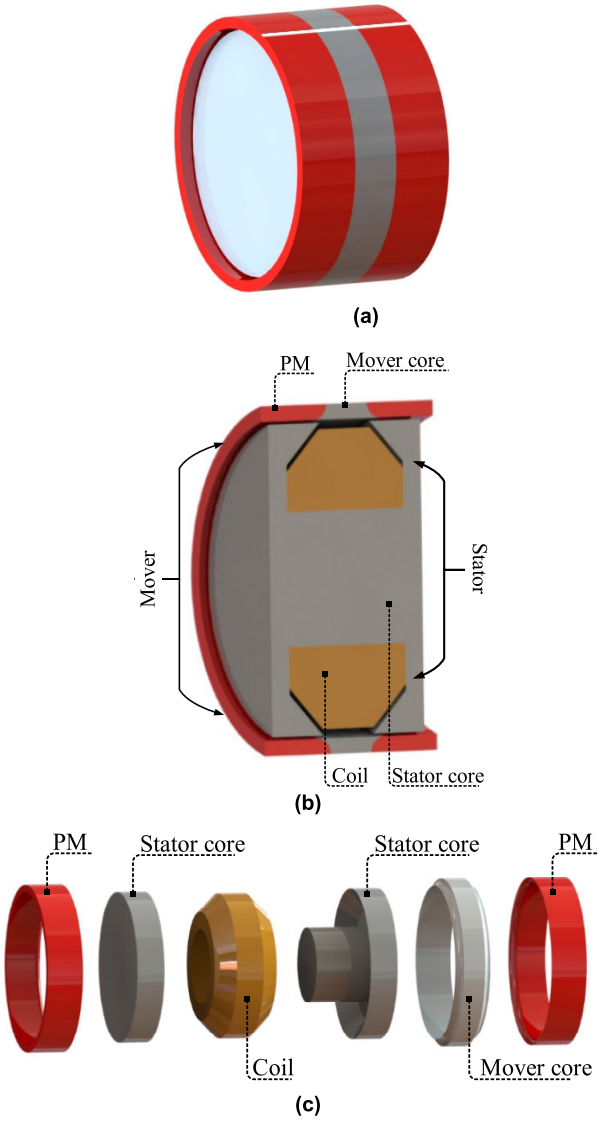

FIGURE 3. CAD model of proposed LOA (a) Full view (b) Section view (c) Exploded view.

parametric sweep and by selecting the optimum value of the parameter. Output parameters like thrust force and stroke are analyzed for direct current (DC) and alternating current (AC) through FEM simulations. Basic conditions for creating electrical and mechanical resonance are analyzed. Detailed analysis of back emf is performed at resonance conditions. Output parameters of the considered LOA are compared with existing LOA which demonstrates improvements in term of motor constant, thrust force and ease in manufacturing.

II. STRUCTURE AND OPERATING PRINCIPLES

A 2-D axisymmetric structure of proposed outer mover inner stator LOA is shown in the (Figure 1). As shown, this topology is composed of two major parts: static and moving. Stator is the static part of the LOA, which is further consist of stator core and winding. A concentrated type winding is wound

TABLE 1. Dimensions of design parameters of proposed LOA.

Symbol	Parameter	Value (mm)
R	LOA radius	60
S_L	Stator length	60
M_L	Mover length	72
SCC_R	Stator center core radius	26
CR_L	Coil radial length	26
C_W	Coil width	46
SL_W	Stator leg width	7
A_G	Air gap	1
PM_L	PM length	28
MC_L	Mover core length	16

around the central core of the stator. Stator core is a wheel shaped part of the LOA. Since Magnetic flux lines are bounce back at the sharp corner of the core, these produce additional reluctance to the magnetic flux. To provide least reluctance path to the flow of magnetic flux, pole-shoes are attached at the end of each stator leg. When the coil is excited by an AC for half cycle of an AC, magnetic flux is produces at one stator leg and leaves from the other. For remaining half cycle, the direction of magnetic flux density becomes opposite as shown in the (Figure 1). Mover that is the moving part of LOA is composed of three parts: two PMs and mover core. PMs are ring structured and axially magnetized. The corners of the PMs at the stator poles are made fillet. The purpose of making fillet PMs is to provide ease in magnetic flux path. The direction of magnetization of both PMs is inward and opposite to one another. Mover core is also ring structured and housed between two PMs. By using parametric sweep, all the geometrical parameters of the proposed LOA are optimized. Values of the optimized geometric parameters of the LOA are shown in (Table 1). For presenting the real view of the LOA, CAD models are shown in (Figure 3), where (Figure 3(a)) shows complete structure of LOA. (Figure 3(b)) and (Figure 3(c)) present section and exploded view of LOA, respectively.

Operating principle of proposed LOA: when the stator winding is energized by an electric current, stator poles (legs) become momentarily magnetized. At one instant, one stator pole yields magnetic field lines and turns as a north pole. Second pole of the stator becomes south pole at the same time. Due magnetic field alignment phenomena, stator second pole receives magnetic flux lines which pass through the mover core. At instant when the direction of the current is inward, mover receives thrust force toward $+z$ direction. Figure 2(a) shows the $+z$ utmost position of the mover where mover is displaced 6 mm toward $+z$ axis. At this moment, right stator pole (leg) becomes south pole and attracts north pole of the PM. The second pole (leg) of the stator becomes as north pole and produces repel force on the mover. Moreover, mover

provides least reactance route to magnetic flux lines receiving by stator. The completed magnetic flux route is represented by an arrow. Similarly, (Figure 2(b)) demonstrates the $-z$ peak point of the mover. At this moment, left stator pole (leg) becomes south pole and attracts north pole of the PM. Also, at this position of the mover, mover provides least reluctance route to magnetic flux lines. When the winding is energized by single phase AC for half cycle of an AC, magnetic field is produced in one direction. At this instant, mover experiences thrust force in one direction. In remaining half cycle of an AC, the direction of magnetic field becomes opposite, and mover experiences thrust force in opposite direction. By continuous supply of a single-phase AC, mover oscillates between two extreme positions called the stroke of the LOA.

III. FEM DESIGN

A 2-D axisymmetric topology of proposed LOA as discussed in section. 2 is built in COMSOL Multiphysics software as shown in (Figure 4). Radial components of the geometry are created in r plan and length of the actuator is built in z plan with same geometric parameters as discussed in previous section. Geometry of the LOA is divided into different region: R_1, R_2, R_3, R_4, R_5, R_6, R_7, R_8 and R_9. R_1 represents the surrounding environment of the actuator and rest of the regions show different portions of the LOA. Material of R_1R_7, R_8 and R_9 are defined as air. Similarly, regions R_2, R_3, R_4, R_5 represent core part of the LOA that is defined as low carbon steel (1010). R_6 represents winding coil and it is defined as copper. In magnetic field module, core regions R_2, R_3, R_4 and R_5 are defined as BH curve constitutive relationship for assigning saturation property. Similarly, the magnetic properties of R_8 and R_9 are defined as remnant flux density. The value of magnetic flux density is kept 1.3 T [1]. The directions of magnetic flux density of R_8 and R_9 are set along $+z$ and $-z$ directions, respectively.

Two types of studies are analyzed: stationary and time dependent. During the stationary analysis, different magnitudes and directions of DC are applied to the coil. Positive value of the DC shows direction of the current into the screen and for negative value of the DC, direction of the DC becomes opposite. Force is calculated on all part of the mover. Two types of graphs, line and point graph are plotted. Data associated with line is plotted on line graphs, like magnetic flux density. Using the same technique, data linked to a point are plotted on point graph like thrust force. Data linked to multiple values of the parameter are analyzed by using parametric sweep option which provides output on each value for the parameter like stroke.

IV. OPTIMIZATION

Optimization of the various geometrical parameters is accomplished by using parametric sweep on a specific parameter. During this optimization process, outer diameter and length of proposed LOA are kept constant. Dimensions of different parameters are varied and select optimum value of the investigated parameter. The dimensions of the parameter are

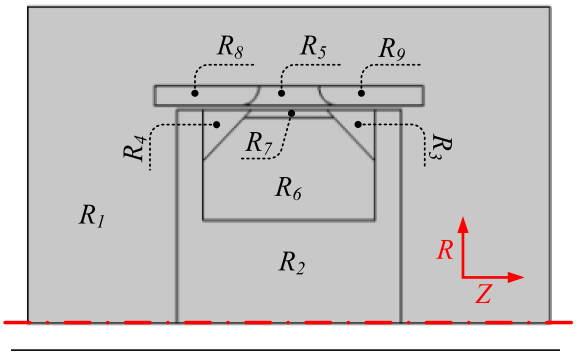

FIGURE 4. FEM design of proposed topology.

compared with output parameter like thrust force experienced by the mover, mover mass and resonance frequency. Similar optimization technique is adopted in [3], [4], [26], where the response of the LOA is analyzed for different values of the parameter.

Figure 5 shows thrust force response for various values of coil radius. LOA radius, length and all other parameters are kept constant during this analysis. Dotted blue arrow in the middle of coil, placed inside the figure, shows the change in coil radius. By increasing coil radial length, number of turns of the coil increases and hence, raise the value of magnetic flux density through stator core. Moreover, magnetic flux density is increased by increasing value of the current. Solid blue and red lines of the figure show thrust force toward $+z$ axis for 5 A and 3 A values of the current, respectively. For 5 A value of the DC current, optimum value of coil radius is 26 mm. Since magnetic flux density also depends on the value of the current and current with value 3 A, optimal value of the coil radius is 30 mm. Similarly, for reverse direction of the current, direction of the thrust force becomes opposite. Doted blue and red lines show thrust force toward $-z$ axis. This response also shows that for 5 A value of the current optimal value of the coil radius is 26 mm. By reducing the value of the current, optimum value of coil radius increases due to saturation effect in core material of the stator. In this process, stator center core radius is also optimized.

Second approach to optimize the proposed LOA is that the thrust force response is recorded for different values of stator tooth (leg) width as shown in (Figure 6). Throughout this analysis, the total length of the stator is kept constant. Thrust force response is verified for both direction of DC and two different magnitudes of DC. Solid blue line shows thrust force response toward $+z$ axis for 5 A value of the input DC. Dotted blue line shows thrust force response for -5 A value of the input DC. Similarly, thrust force is plotted for 3 A and -3 A values of the current depicted by solid and dotted red lines respectively. Mover position at this moment is the Mean position. In this process, stator tooth width (leg) is optimized. Consequently, another parameter called coil width is also optimized in this process. This figure also presents that thrust force is optimized toward both directions of the mover.

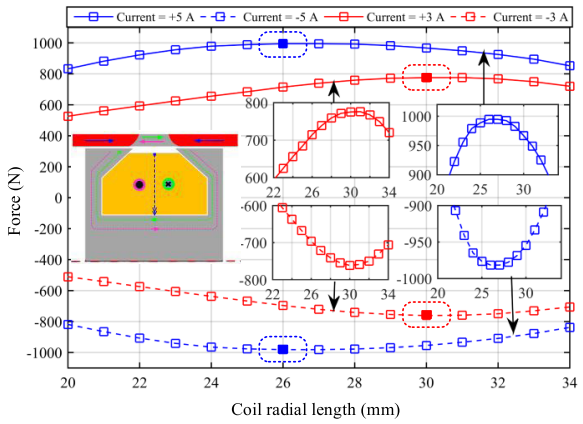

FIGURE 5. Coil radial length optimization.

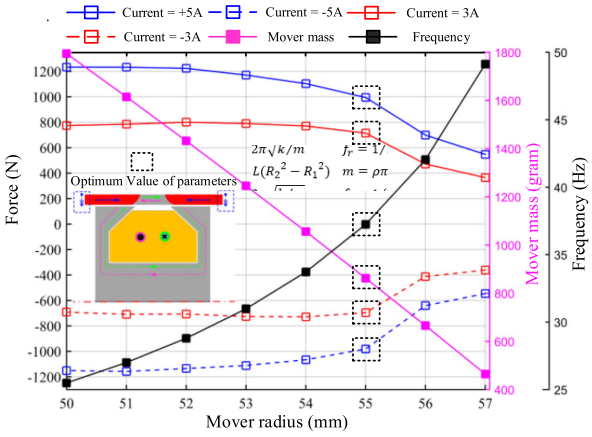

FIGURE 7. Mover radius optimization.

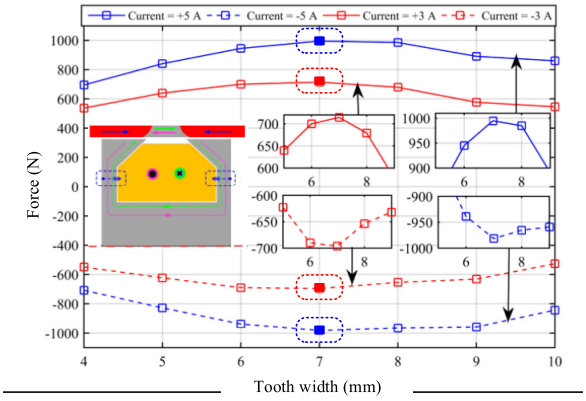

FIGURE 6. Stator tooth (leg) width optimization.

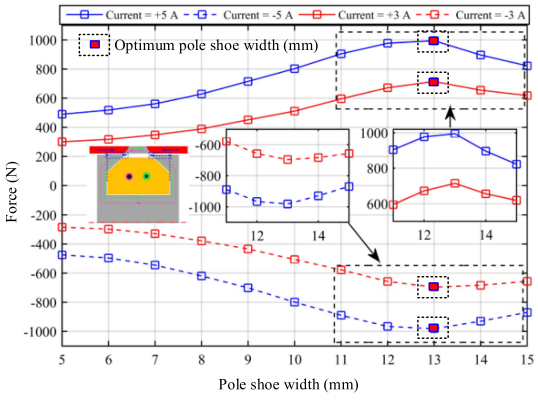

FIGURE 8. Pole shoe width optimization.

This analysis reveals that optimum value of the stator tooth width is 7 *mm*.

Reduction of the mover mass shows significant effect on resonance frequency which leads to improve output power of the LOA. Since mover mass is the design parameter of LOA, it cannot reduce any more. Figure 7 shows the relationship of mover inner radius with thrust force, mover mass and operating resonance frequency. Outer radius R_2 of the LOA is kept constant while inner radius R_1 of the mover and stator radius are dynamic in this optimization process. Solid and doted, blue and red lines show effect of mover inner radius on thrust force of the LOA for DC of value 5 A, -5 A, 3 A and -3 A respectively. From Figure 7, it is clear that there is considerable decrease in thrust force after mover inner radius of value 55 *mm*. By increasing the value mover inner radius, thickness of the mover reduces thereby decreasing mover mass. In this figure pink line shows the attenuation of mover mass due to increase in mover inner radius. The calculated value of the mover mass of the LOA at 55 *mm* inner radius of the mover is 901 grams, whereas outer radius of the LOA is 60 *mm*. Since resonance frequency is calculated by moving mass and spring stiffness, 60 *kN/m* value of the spring constant resonance frequency results in 41 *Hz*. Furthermore, utilization of PM volume is also optimized in optimization procedure.

Like previous optimization technique, pole shoe width is also optimized by verifying its response in term of thrust force. During this optimization, dimension of the pole shoe is varied toward the coil. Only coil chamfer dimension is varied, while all other parameters of the LOA are kept constant. Figure 8 presents thrust force experienced by mover at different values of pole shoe width for both directions of the current. Since stroke of the LOA is dependent on pole width of the actuator, stroke of the LOA is also optimized on account of this procedure. This figure presents that optimum thrust force is achieved if the value of the pole shoe width is 13 *mm*.

V. FEM STATIC ANALYSIS (RESULTS AND DISCUSSIONS)

Figure 9 shows the simulated view of the proposed LOA when the coil is excited with DC of magnitude 5 A. Direction of magnetic flux density is expressed by an arrow that is based on the direction of the current. Figure 9(a) shows the simulated view when the direction of current is inward while in (Figure 9(b)) the direction of the current is outward. In (Figure 9(a)), the direction of the force acting is left to right. In other words, the direction of force is toward +z axis. Similarly, in (Figure 9(b)) the direction of the force is from right to left or toward +z axis. Legend shows the amount of magnetic flux at various locations of the proposed LOA.

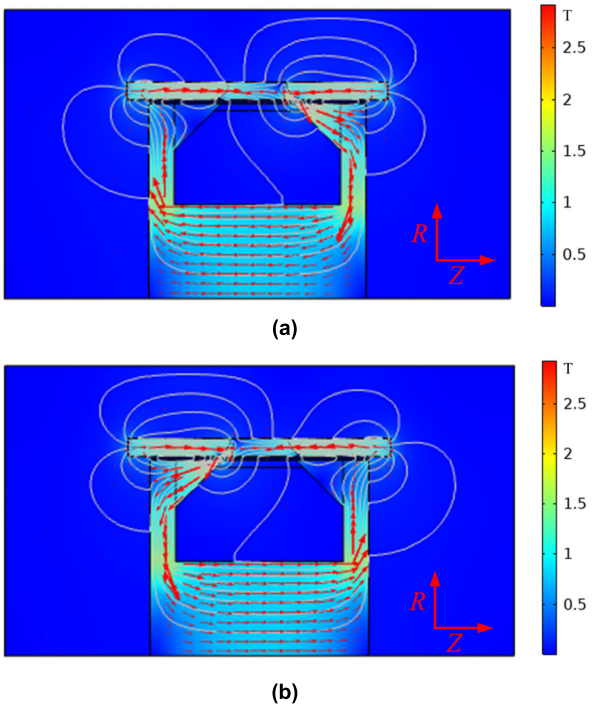

FIGURE 9. Simulated view of the proposed LOA (a) Direction of the current is outward (b) Direction of the current is inward.

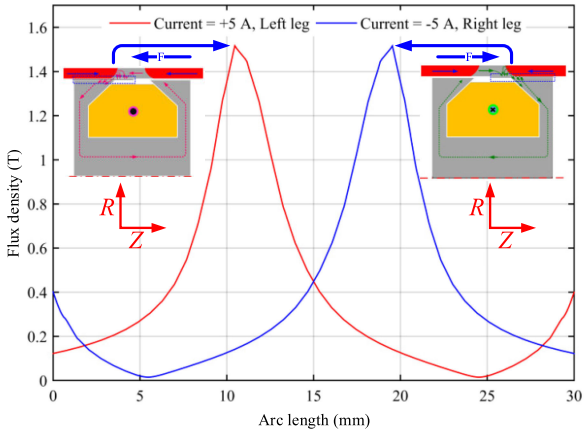

FIGURE 10. Line graph of magnetic flux density measured in front of stator leg.

Magnetic flux density is measured in air gap opposite to the stator poles. Figure 10 shows the magnitude of magnetic flux density (MFD) entering from mover to stator on both directions of the current. Red line of the figure shows magnitude of MFD entering from mover to left stator leg. At this instant, direction of the current is outward and mover experiences thrust force toward −z axis, allowing more flux from mover to stator. Similarly, when the direction of the current becomes opposite, direction of magnetic flux density gets reverse. Blue line shows magnitude of MFD receiving by stator at right stator leg of the LOA. At this instant, mover tends to move toward +z axis, allowing more flux from mover to stator. Thus, bidirectional MFD and thrust force are produced if the stator coil is excited by a single-phase alternating supply.

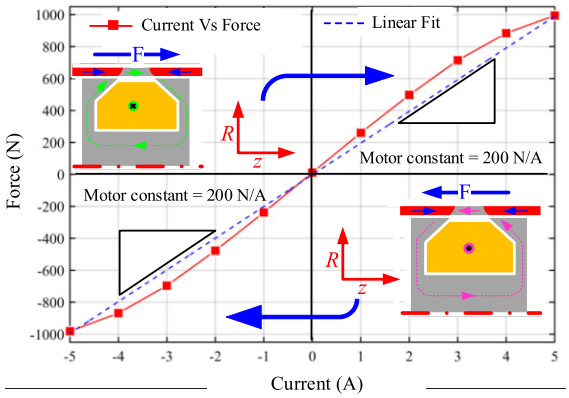

FIGURE 11. Thrust force response on different values of DC.

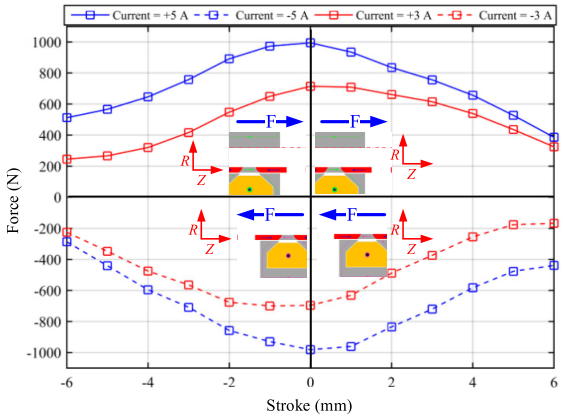

FIGURE 12. Thrust force on different position of the mover.

Thrust force performance of the investigated LOA for discrete values of the DC is shown in the (Figure 11). In this figure, red line shows thrust force response toward +z and −z axis at mean position of mover. DC of range −5 A to 5 A is supplied to the winding (coil) and response of the mover in term of thrust force is plotted in the figure. From the figure, it is obvious that there is direct relation between magnitude of the DC and thrust force. Slop of linear fit shows the average change in the magnitude of thrust force due to change in the magnitude of DC. Slop of the line called motor constant is 200 N/A. Variation in the value of thrust force is reduced at higher value of the DC. This reduction in variation is due to saturation of the core materials at higher value of the current. The same way by altering the direction of the DC (0 to −5 A) direction of the thrust force becomes reversed. Thrust force shown by third quadrant of (Figure 11) is the force experienced by the mover when direction of the current becomes opposite. Negative value of the thrust force shows the direction of the force toward −z axis. Proposed LOA shows identical thrust force and motor constant in both directions (toward +z and −z) of the thrust force.

Thrust force response on distinct values of the stroke is shown in (Figure 12). Solid blue and red lines show thrust force response for input 5 A and 3 A value of the DC while

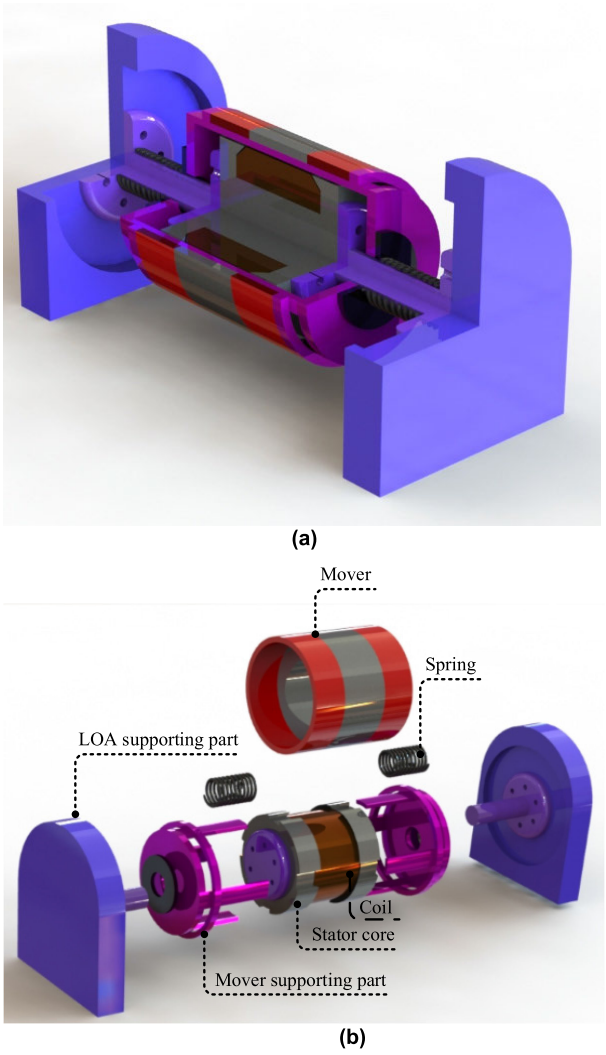

FIGURE 13. Complete assembly of proposed LOA (a) Section view (b) Exploded view.

dotted blue and red lines show thrust force response for −5 A and −3 A values of the input DC, respectively. This figure shows thrust response force for both directions of the DC. For better understanding, this figure is divided in to 4 quadrants. Force associated with second quadrant helps to displace mover from −z peak point to mean position. First quadrant shows thrust force that helps displacing the mover from mean position to +z peak point. Similarly, force associated with third and fourth quadrant are opposite in direction to force shown in first and second quadrant. This force helps displacing the mover from +z peak point to mean position and furthermore to −z peak point. From the figure, it is clear there is exact contrary response of thrust force when the direction of the current is altered. This figure concludes that stroke of the proposed LOA is 12 *mm*.

VI. RESONANCE

Linear oscillating actuator reveals great advancement over conventional actuation technique. Operation at resonance condition is one of these improvements. Most of the linear

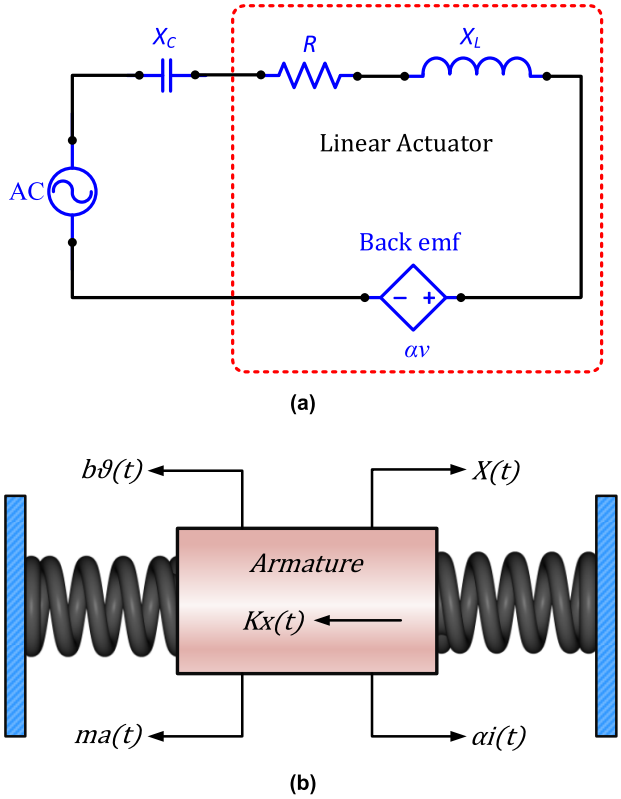

FIGURE 14. (a) Equivalent electrical circuit model of LOA (b) Mechanical model of LOA.

actuators are operated at resonance frequency. There are two types of resonance conditions: mechanical resonance and electrical resonance that can be achieved in LOA. Significant parameter that influences the performance of the actuator is the highest value of the operating frequency [23]. Resonance frequency is increased by reducing the mass of the mover. The main obstacle in the design of LOA is the reduction of the mover mass [4]. Rising the value of the resonance frequency shows significant effect on output power of the actuator. Furthermore, increasing the value of the operating frequency reduces required external capacitance to achieve electrical resonance. Operation at resonance are achieved by exciting the coil at mechanical resonance frequency. At resonance frequency, very less electromagnetic force is needed to perform its operation [5]. Furthermore, minimum electric current is passed through coil, which yields minimum ohmic loses. Efficiency of the actuator is high at resonance condition due to small input power [11]. Figure 13 shows the complete assembly of proposed LOA. Figure 13 (a) shows the section view where mover is attached to the two resonant springs. Mover is placed on mover support which is further attached to the supporting rods. Figure 13(b) shows exploded view of the assembly where every part of the assembly is shown in its real view.

A. MECHANICAL RESONANCE

Operation at resonance is a key parameter which improves efficiency of the LOA. Mechanical resonance is achieved by

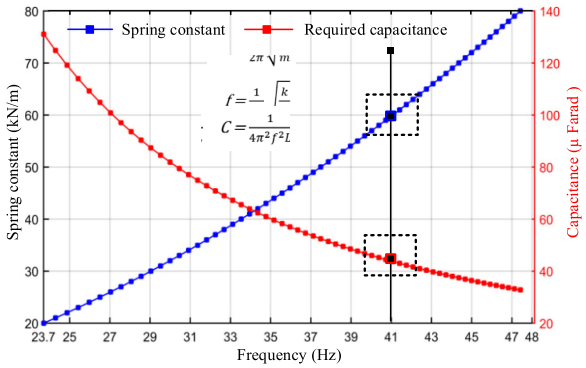

FIGURE 15. Resonant frequencies versus spring constant and required capacitance.

operating LOA at mechanical resonance frequency. Mechanical resonance frequency is determined by mover mass and spring stiffness. Mover mass cannot be reduced to a great extent, while springe stiffness of required value can be selected. To match the value of mechanical resonance frequency with electrical resonance frequency, required magnitude of spring stiffness can be selected. Mechanical spring stores and releases energy when required to the system. Actuator at resonance oscillates in the range of required stroke while utilizing minimum electromagnetic force. Amplitude and frequency of the input alternating voltage control the magnitude of the stroke and number of oscillations per unit time, respectively. LOA operation at resonance condition makes the actuator secure from excessive reactive current [24]. The relationship of resonant frequency with moving mass and spring stiffness is given by

$$f = \frac{1}{2\pi}\sqrt{k}/m \tag{1}$$

In (1) f is the operating resonance frequency, m is the mover mass and k is the spring stiffness. From this relationship it is clear that there is inverse relation between mover mass and operating frequency.

B. ELECTRICAL RESONANCE

LOA is a series circuit of resistance R, inductance L and back electromotive force as shown in (Figure 14 (a)). Single phase AC source is used to supply input loading to the actuator. Back electromotive force is determined by motor constant α and mover velocity $\dot{x}$. Mover velocity is calculated by operating frequency and stroke of the LOA. Resistance R and inductive reactance X_L are the design parameters of LOA which depend on number of turns of coil. Number of turns are determined from wire gauge used. For creating electrical resonance, an external capacitor X_C is attached in series. The purpose of creating electrical resonance is to cancel out inductive reactance X_L by capacitive reactance X_C and applied voltage is built across the resister. Impedance of the circuit becomes less at electrical resonance; hence, input power of actuator is reduced. Formula for determining required capacitance to create electrical resonance is given by

$$C = \frac{1}{4\pi^2 f^2 L} \tag{2}$$

In (2), f is the operating frequency in Hz. L is the inductance of the coil and C is the required external capacitance of capacitor.

Using equation (1), resonant frequency of proposed LOA is plotted for different values of spring constant using mover mass of 901 grams as discussed in section 4 (Figure 15) shows values of resonant frequency for different values of spring constant. Since required capacitance for creating electrical resonance is a function of operating frequency, using equation (2) required capacitance is plotted for distinct values of mechanical resonant frequencies. This figure concludes that for springs of stiffness 60 kN/m mechanical resonance frequency of the LOA is 41 Hz and required capacitance of creating electrical resonance is 43 μF.

TABLE 2. Electrical and mechanical parameters of the LOA.

Parameter	Symbol	Value
Coil resistance	R	3.6 Ω
Coil inductance	L	343.7 mH
Motor constant	α	200 N/A
Spring constant	k	60 kN/m
Damping coefficient	b	7 Ns/m
Mover mass	m	0.901 k g

VII. ANALYTICAL MODELLING OF BACK EMF

Electric circuit model of the actuator shown in (Figure 14 (a)) is a series RLC circuit that is evaluated in (3) where v_{exc} is the applied excitation voltage of specific magnitude and frequency, R and L are the resistance and inductance of the coil, respectively. v_{bemf} which is equivalent to $\alpha\vartheta$, α is the back emf coefficient and ϑ is mover velocity. Time dependent current $i(t)$ passing through coil that flows due to voltage across the winding.

$$v_{exc(t)} = Ri(t) + L\frac{di}{dt} + \frac{1}{C}\int i(t)\,d(t) + v_{bemf} \tag{3}$$

Solving (3) in Laplace domain, amount of current flowing through coil is evaluated by

$$I = \frac{(V_{exc} - V_{bemf})s}{Rs + Ls^2 + \omega_{ne}^2 L} \tag{4}$$

where electrical resonance frequency is $\omega_{ne} = 1/\sqrt{LC}$. Mechanical model of the LOA as shown in fig. 14 (b)

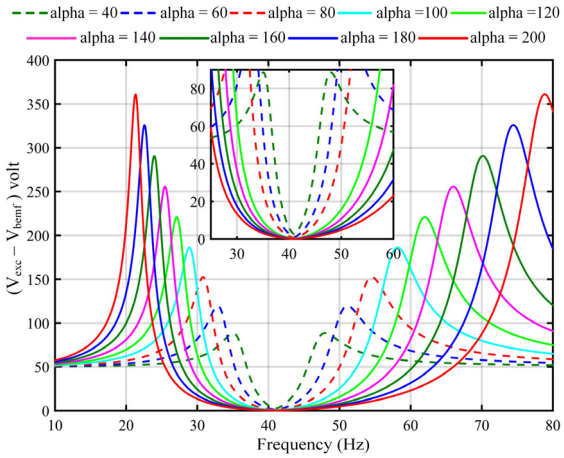

FIGURE 16. Voltage difference for different frequencies and motor constant.

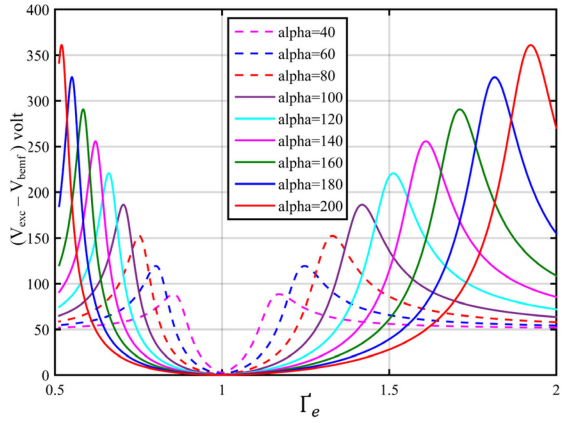

FIGURE 17. Voltage difference for different Γ_e and motor constant.

and its equivalent force model acting on the mover is derived as

$$\alpha i\,(t) = ma(t) + b\vartheta(t) + Kx(t) \tag{5}$$

where $\alpha i\,(t)$ is the electromagnetic force, $ma(t)$ is the inertial force, $b\vartheta(t)$ is the damping force and $Kx(t)$ is the spring force. $m, a\,(t), b, \vartheta\,(t), K, x(t)$ are the mover mass, acceleration, spring damping coefficient, mover velocity, spring constant and mover displacement, respectively. Motor constant is as the amount electromagnetic thrust per unit current. Evaluating (5) in Laplace domain, expression for the current is as

$$I = \frac{\vartheta}{s\alpha}\left(ms^2 + bs + m\omega_{nm}^2\right) \tag{6}$$

where $\omega_{nm} = \sqrt{k}/m$ is the mechanical resonant frequency (MRF). Back emf constant Vs/m used in (3) and motor constant N/A shows identical response in electrical and mechanical system; hence, α is used for both back emf constant and motor constant used in (3) and (5) [6]. Since current through a coil is flowing due to difference of exciting voltage and back emf. Differences in these voltages are derived

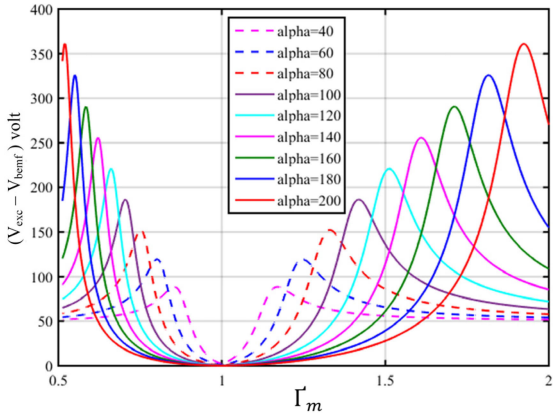

FIGURE 18. Voltage difference for different Γ_m and motor constant.

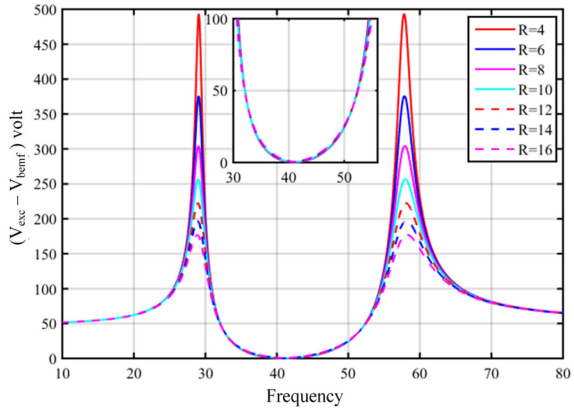

FIGURE 19. Voltage difference for different frequencies and multiple values of coil resistance.

using (4) and (6).

$$\begin{aligned} V_{exc} - V_{bemf} &= \frac{\vartheta}{\alpha}\left[s^2Lm + s\,(Rm + bL)\right. \\ &\left. + \frac{1}{s}\left(mR\omega_{nm}^2 + bL\omega_{ne}^2\right) + \frac{1}{s^2}mL\omega_p^2 + mL\omega_t^2 + bR\right] \end{aligned} \tag{7}$$

where $V_{exc} - V_{bemf}$ is the difference between excited voltage and back emf while $\omega_p^2 = \omega_{nm}^2\omega_{ne}^2$ and $\omega_t^2 = \omega_{nm}^2 + \omega_{ne}^2$. Solving (7) in frequency domain, expression for voltages difference is

$$V_{diff} = \frac{\vartheta}{\alpha}\left[bR - mL\omega^2\delta_m\delta_e + j\omega\,(mR\delta_m + bL\delta_e)\right] \tag{8}$$

where $V_{diff} = V_{exc} - V_{bemf}$, $\delta_m = 1 - \Gamma_m^2$ and $\delta_e = 1 - \Gamma_e^2$. Γ_m is the ration of MRF to the applied frequency while Γ_e is the ratio of ERF to the applied frequency. Magnitude of voltage difference V_{diff} is

$$\left|V_{diff}\right| = \frac{\vartheta}{\alpha}\sqrt{b^2R^2 + m^2\omega^2\delta_m^2Z_e + L^2\omega^2\delta_e^2Z_m} \tag{9}$$

Parameters related to mechanical design of the LOA is represented by $Z_m = b^2 + m^2\omega^2\delta_m^2/2$, while other parameters

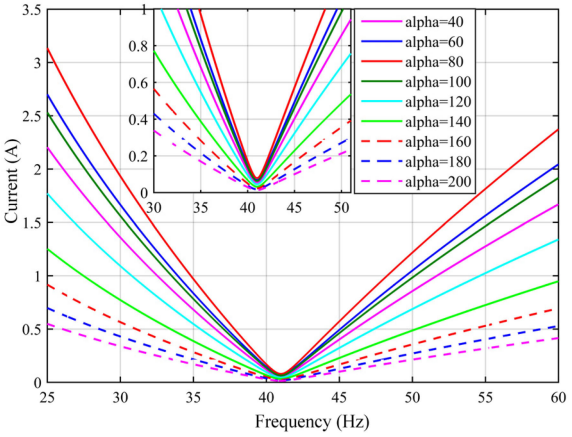

FIGURE 20. Current though coil at different values of excitation frequencies.

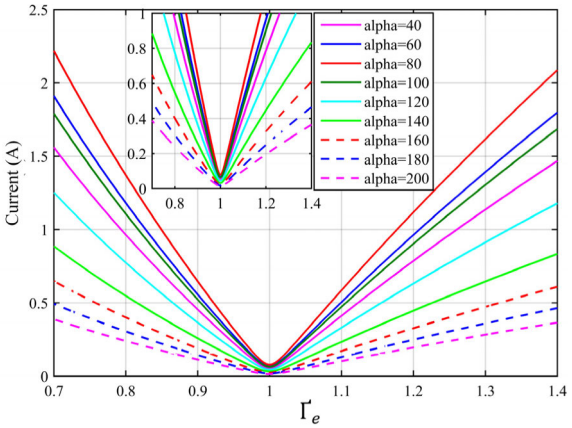

FIGURE 21. Current though coil at different values of Γ_e.

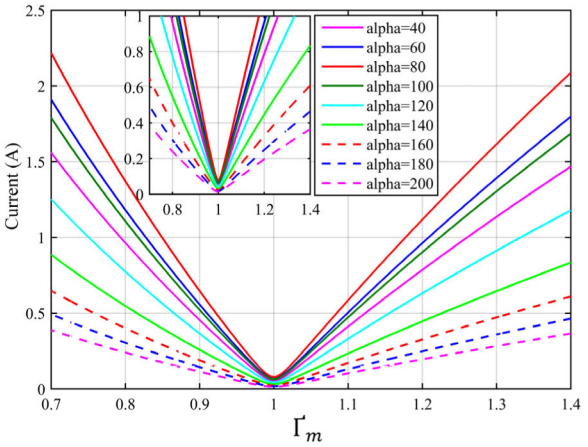

FIGURE 22. Current though coil at different values of Γ_m.

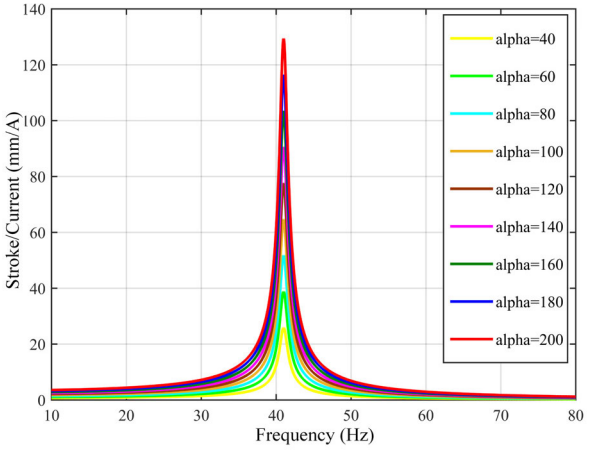

FIGURE 23. Stroke to current ratio at different values of excitation frequencies.

related to electrical design of the LOA are symbolized by $Z_e = R^2 + L^2\omega^2\delta_e^2/2$. Mover velocity ϑ used in (9) is studied in [25] is given by

$$\begin{aligned} |\vartheta| &= \frac{|V|\,\alpha\omega^2}{\sqrt{\Upsilon^2 + \Psi^2}} \\ \Upsilon &= mL\omega^2\left(1-\Gamma_e^2\right)\left(1-\Gamma_m^2\right) - \omega^2(bR+\alpha^2) \\ \Psi &= -mR\omega^3\left(1-\Gamma_m^2\right) - bL\omega^3(1-\Gamma_e^2) \end{aligned} \tag{10}$$

At resonance frequency, minimum electromagnetic force and current are required for proper operation. In order to estimate amount of current, equation is given by

$$|I| = \frac{|V|\,\omega^2}{\sqrt{\Upsilon^2 + \Psi^2}}\sqrt{b^2 + \zeta_m^2} \tag{11}$$

where $\zeta_m = \omega m(1-\Gamma_m^2)$ and $|V|$ is the magnitude of voltage applied. This equation produces minimum value of the current at resonance frequency. Damping coefficient b is a design parameter that can be adjusted by thickness of wire, material used, length of the spring etc. Stroke of the LOA is also one of the important output parameters of the LOA. Higher the value of the stoke, more amount of gas compression will be achieved. Stroke is also resonance frequency dependent parameter. Formula for stroke to current ratio is specified by

$$\frac{x}{I} = \frac{\alpha}{\omega\sqrt{b^2 + \zeta_m^2}} \tag{12}$$

Stroke to current ratio of (12) has high value at resonance frequency. At high value of stroke to current ratio, the value of stroke is high while the value of the current will be smaller.

Circulation of current through a coil is the result of voltage difference across the winding, and this difference is the variance between the excitation voltage and back *emf*. Figure 16 shows the difference between excitation voltage and back emf for different values of excitation frequencies using (9). From the figure, it is obvious that there is minimum difference between excitation voltage and back emf at resonance frequency. Furthermore, this process is repeated for different values of motor constant which shows that for higher values of the motor constant there is an increase in resonance frequency range. At frequencies other than resonance frequency, there is large value of voltage difference. These spikes are due to inductive nature of the coil. This figure concludes that at resonance frequency voltage through coil is minimum.

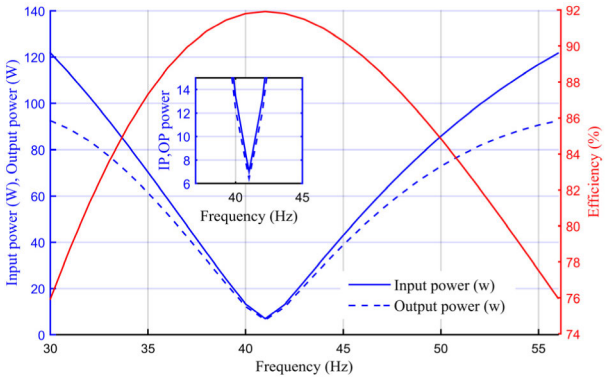

FIGURE 24. Calculated values of input power, output power and efficiency of the proposed LOA.

Procedure adopted in (Figure 16) is repeated for $\Gamma_e = \omega_{ne}/\omega$ in (Figure 17). In this figure, voltage difference is plotted for various values of Γ_e and motor constant that presents that there is minimum voltage difference when excitation frequency ω is equal to ERF ω_{ne}. This investigation presents that operating LOA at ERF there will be least voltage difference through coil. Moreover, effect of motor constant is also analyzed which shows same effect as discussed in previous analysis.

Furthermore, effect of mechanical resonance is analyzed in (Figure 18). In this figure, voltage difference is investigated for different values of $\Gamma_m = \omega_{nm}/\omega$ and motor constant. This figure presents that at mechanical resonance condition voltage difference through coil is least. By increasing value of motor constant, range of Γ_m increases which increases the range of operating frequencies at fixed MRF. Figure 16, 17 and 18 conclude that voltage through coil is built up with least magnitude by operating LOA at resonance conditions.

Winding resistance depends on wire diameter and length. Figure 19 investigates voltage difference for different frequencies and wire resistance. From the figure, it is clear there is no effect of wire resistance on resonant frequency. Whereas, spikes in voltage difference due inductive nature of the coil is high for small value of resistance.

Since current passes through coil is due to voltage across the winding, and this voltage is in real the voltage difference between excitation voltage and back emf. Previously, it is described that at resonant frequency there is least voltage difference across the coil. Due to minimum voltage difference, current passing through coil will be minimum. Figure 20 shows current passing though coil at different values of excitation frequencies and motor constant using (11). From this figure it is obvious that shifting the value of excitation frequency toward the resonant frequency there is significant decreases in current magnitude. Moreover, it is also shown that current change for lower value of motor constant is high, whereas for high value of motor constant change in current due to change in frequency is smaller. At resonance frequency $41Hz$, current approaches to zero. This analysis concludes that at resonance frequency input loading to the LOA is minimum which will further improve the efficiency of LOA.

Same procedure is repeated for electrical resonance and mechanical resonance conditions in (Figure 21, 22), respectively. At electrical resonance condition, the ratio Γ_e is equal to unity and figure shows that at $\Gamma_e = 1$ there is minimum current passing through coil. Moreover, effect of motor constant is same as discussed in previous figure.

Similarly, at mechanical resonance condition $\Gamma_m = 1$, there is minimum current passing though coil as shown in (Figure 22). Hence, at mechanical resonance input, power to the LOA is minimum. Both electrical and mechanical resonance are achieved by operating the LOA at 41Hz frequency of the input alternating source. These figures further validate the resonance phenomena in term of coil current.

Stroke to current ratio of LOA is analyzed for different values of frequencies in (Figure 23), using (12). In this figure, stroke to current ratio is analyzed for different values of excitation source frequencies and motor constants. At resonance frequency, magnitude of Stroke to current ratio is maximum as compared to other frequencies of excitation source. Moreover, motor constant also plays great role at resonance frequency in term of stroke to current ratio. Higher the value of motor constant, stroke to current ratio of the LOA is high. Since for the high value of the stoke, output power of the LOA improves that will further increase the efficiency of the LOA. This analysis concludes that, operating the LOA at resonance condition reduces input power and improves output power that leads to improving efficiency of the LOA.

Efficiency of the proposed LOA is calculated using mathematical formulas of electromagnetic force, velocity, current and applied voltage, as discussed in [6]. The effect of resonance condition on these parameters are investigated. Input power to the LOA is determined by using the product of the applied voltage and current passing through the coil, while output power of the LOA is calculated by multiplying the electromagnetic force and velocity of the mover. Response of the LOA in terms of input power and output power is presented in (Figure. 24). This figure presents both input and output power of the LOA which is minimum at resonance frequency. Furthermore, difference between input power and output power is also minimum at resonance frequency, resulting in high efficiency. Beyond the resonance frequency, difference between the powers increases which reduces the value of the efficiency.

VIII. COMPARISON WITH CONVENTIONAL DESIGNS OF LOA

Comparison of proposed LOA with conventional designs of LOA in terms of mover structure, volume, stroke and motor constant is shown in (Table 2). Topology discussed in [2] is moving iron (solenoid) which produces unidirectional thrust force. This design is operated by pulsating DC. Complete oscillation is made possible by using a resonant spring attached to the mover of LOA. The stroke of this design is 23 *mm*, which is more than enough for compressor

TABLE 3. Comparison of design and output parameters of proposed LOA with conventional designs of LOA.

Ref. No	Moving type	Volume (mm3)	Stroke (mm)	Thrust/Kg of PM N/m^3	Motor constant N/A
[1]	Moving magnet	6.6×10^5	13	Ferrite PMs	73.3
[2]	Moving Iron	1.54×10^6	23	No PM	14
[4]	Moving magnet	7.88×10^5	14	163.246	34.6
[6]	Moving magnet	1.73×10^6	8.8	146.957	38
[8]	Moving magnet	7.7×10^5	10	147.761	48
[15]	Moving magnet	2.72×10^5	14	254.799	56.6
[23]	Moving magnet	8.26×10^5	12	108.606	55
Proposed LOA	Moving magnet	6.8×10^5	12	263.744	200

in refrigeration system. Motor constant of this design is very small (14 N/A). This design produces very less electromagnetic force while volume of this topology is high. Design considered in [4] produces bidirectional thrust force and the stroke of oscillation is 14 mm. This design consists of moving magnet with axially magnetized PMs used. Motor constant of this design is 34.6 N/A. Structure used in [6] is the moving magnet with radially magnetized PMs embedded on the mover. Main defect of this design is complex mover structure. This topology produces reciprocating thrust force with stroke 8.8 mm. Motor constant of this design is 38 N/A. Moving magnet LOA used in [8] produces linear oscillation with stroke 10 mm and motor constant 48 N/A. Proposed LOA has a stoke 12 mm and motor constant 200 N/A. Improvement in motor constant is great achievement of this design. Moreover, thrust force response of proposed topology is very high. Furthermore, operating resonance frequency of proposed is also feasible of refrigeration system application.

IX. CONCLUSION

An outer mover moving magnet topology of LOA for compressor in refrigeration system is proposed in this paper. Axially magnetized tubular magnet is used that is placed in opposite direction of magnetization. 2-D axisymmetric topology is used for indicating flux path and elaborating operation principles. CAD model is shown for better understanding of the proposed topology. Parametric study is focused where all the design, input and output parameters are analyzed in detail. Design parameters like coil radius, stator leg width and pole shoe length are investigated in term of output parameter called thrust force. Mover radius is analyzed in term of thrust force, mover mass and resonant frequency. Rest of the parameters are optimized by the same method. Static analysis is performed through FEM for investigating motor constant and stroke of the proposed LOA. Basic conditions for creating electrical and mechanical resonance are explained. Detailed analysis of back emf and coil current at resonance condition is performed analytically. Proposed LOA is compared with conventional designed LOA that shows significant development in motor constant, thrust force and ease in fabrication.

REFERENCES

[1] C.-W. Kim, G.-H. Jang, S.-W. Seo, I.-J. Yoon, S.-H. Lee, S.-S. Jeong, and J.-Y. Choi, "Comparison of electromagnetic and dynamic characteristics of linear oscillating actuators with rare-Earth and ferrite magnets," *IEEE Trans. Magn.*, vol. 55, no. 7, pp. 1–4, Jul. 2019.

[2] A. Bijanzad, A. Hassan, and I. Lazoglu, "Analysis of solenoid based linear compressor for household refrigerator," *Int. J. Refrig.*, vol. 74, pp. 116–128, Feb. 2017.

[3] J. Wang, D. Howe, and Z. Lin, "Design optimization of short-stroke single-phase tubular permanent-magnet motor for refrigeration applications," *IEEE Trans. Ind. Electron.*, vol. 57, no. 1, pp. 327–334, Jan. 2010.

[4] Z. Ahmad, A. Hassan, F. Khan, and I. Lazoglu, "Design of a high thrust density moving magnet linear actuator with magnetic flux bridge," *IET Electr. Power Appl.*, vol. 14, no. 7, pp. 1256–1262, Jul. 2020.

[5] A. Bijanzad, A. Hassan, I. Lazoglu, and H. Kerpicci, "Development of a new moving magnet linear compressor. Part A: Design and modeling," *Int. J. Refrig.*, vol. 113, pp. 70–79, May 2020.

[6] A. Hassan, A. Bijanzad, and I. Lazoglu, "Dynamic analysis of a novel moving magnet linear actuator," *IEEE Trans. Ind. Electron.*, vol. 64, no. 5, pp. 3758–3766, May 2017.

[7] U. Birbilen and I. Lazoglu, "Design and analysis of a novel miniature tubular linear actuator," *IEEE Trans. Magn.*, vol. 54, no. 4, pp. 1–6, Apr. 2018.

[8] P. Immonen, V. Ruuskanen, and J. Pyrhönen, "Moving magnet linear actuator with self-holding functionality," *IET Elect. Syst. Transp.*, vol. 8, no. 3, pp. 182–187, Feb. 2018.

[9] Q. Lu, M. Yu, Y. Ye, Y. Fang, and J. Zhu, "Thrust force of novel PM transverse flux linear oscillating actuators with moving magnet," *IEEE Trans. Magn.*, vol. 47, no. 10, pp. 4211–4214, Oct. 2011.

[10] E. Sayed, Y. Yang, B. Bilgin, M. H. Bakr, and A. Emadi, "A comprehensive review of flux barriers in interior permanent magnet synchronous machines," *IEEE Access*, vol. 7, pp. 149168–149181, 2019.

[11] K. Liang, "A review of linear compressors for refrigeration," *Int. J. Refrig.*, vol. 84, pp. 253–273, Dec. 2017.

[12] C. Pompermaier, N. Sadowski, A. Zambonetti, M. V. F. da Luz, and F. J. H. Kalluf, "Performance analysis of a tubular linear motor applied in compressors," in *Proc. 5th IET Int. Conf. Power Electron., Mach. Drives (PEMD)*, 2010, p. 243.

[13] K. H. Kim, H. I. Park, S. S. Jeong, S. M. Jang, and J. Y. Choi, "Comparison of characteristics of permanent-magnet linear oscillating actuator according to laminated method of stator core," *IEEE Trans. Appl. Supercond.*, vol. 26, no. 4, pp. 1–4, Jun. 2016.

[14] C. Pompermaier, K. Kalluf, A. Zambonetti, M. V. Ferreira da Luz, and I. Boldea, "Small linear PM oscillatory motor: Magnetic circuit modeling corrected by axisymmetric 2-D FEM and experimental characterization," *IEEE Trans. Ind. Electron.*, vol. 59, no. 3, pp. 1389–1396, Mar. 2012.

[15] J. Sun, C. Y. Luo, and S. Xu, "Improvement of tubular linear oscillating actuators by using end ferromagnetic pole pieces," *IEEE Trans. Ener. Conver.*, vol. 33, no. 4, pp. 1686–1691, Dec. 2018.

[16] X. Chen and Z. Q. Zhu, "Analytical determination of optimal split ratio of E-core permanent magnet linear oscillating actuators," *IEEE Trans. Ind. Appl.*, vol. 47, no. 1, pp. 25–33, Jan. 2011.

[17] F. Marignetti and M. Scarano, "Comparative analysis and design criteria of permanent magnet tubular actuators," *Electr. Eng.*, vol. 84, no. 5, pp. 255–264, Dec. 2002.

[18] M. Petrun and S. Steentjes, "Iron-loss and magnetization dynamics in non-oriented electrical steel: 1-D excitations up to high frequencies," *IEEE Access*, vol. 8, pp. 4568–4593, 2020.

[19] H.-K. Yeo and J.-S. Ro, "Novel analytical method for overhang effects in surface-mounted permanent-magnet machines," *IEEE Access*, vol. 7, pp. 148453–148461, 2019.

[20] S. Miric, P. Kuttel, A. Tuysuz, and J. W. Kolar, "Design and experimental analysis of a new magnetically levitated tubular linear actuator," *IEEE Trans. Ind. Electron.*, vol. 66, no. 6, pp. 4816–4825, Jun. 2019.

[21] O. Gomis-Bellmunt, F. Ikhouane, P. Castell-Vilanova, and J. Bergas-Jané, "Modeling and validation of a piezoelectric actuator," *Electr. Eng.*, vol. 89, no. 8, pp. 629–638, Aug. 2007.
[22] L. Pîslaru-Dănescu, A. M. Morega, M. Morega, F. Bunea, P. Marius, and C. A. Băbuţanu, "A new type of linear magnetostrictive motor," *Electr. Eng.*, vol. 99, no. 2, pp. 601–613, Jun. 2017.
[23] H. Liang, Z. Jiao, L. Yan, L. Zhao, S. Wu, and Y. Li, "Design and analysis of a tubular linear oscillating motor for directly-driven EHA pump," *Sens. Actuators A, Phys.*, vol. 210, no. 4, pp. 107–118, Apr. 2014.
[24] Z. Zhang, K. W. E. Cheng, and X. D. Xue, "Study on the performance and control of linear compressor for household refrigerators," in *Proc. 5th Int. Conf. Power Electron. Syst. Applications (PESA)*, Dec. 2013, pp. 1–4.
[25] A. Hassan, A. Bijanzad, and I. Lazoglu, "Electromechanical modeling of a novel moving magnet linear oscillating actuator," *J. Mech. Sci. Technol.*, vol. 32, no. 9, pp. 4423–4431, Sep. 2018.
[26] N. Ahmad, F. Khan, H. Ali, S. Ishaq, and E. Sulaiman, "Outer rotor wound field flux switching machine for in-wheel direct drive application," *IET Electr. Power Appl.*, vol. 13, no. 6, pp. 757–765, 2019.

ZAHOOR AHMAD was born in Khyber Pakhtunkhwa, Pakistan, in 1993. He received the B.S. degree in electrical engineering from the University of Science and Technology, Bannu, Khyber Pakhtunkhwa, in 2016, and the M.S. degree in electrical engineering from COMSATS University Islamabad at Abbottabad, Pakistan. He worked on research exchange program with the Electrical Machine and Drive Laboratory, GIK Institute, for more than one year. His research interests include design of permanent magnet motors, actuator, and helical motors.

ADNAN HASSAN (Member, IEEE) was born in Pakistan, in 1983. He received the B.Eng. degree in mechatronics engineering from the National University of Sciences and Technology (NUST), Islamabad, Pakistan, in 2006, and the Ph.D. degree in mechanical engineering from Koç University, Istanbul, Turkey, in 2017.

From 2007 to 2012, he was a Research Engineer with the National Engineering and Scientific Commission, Islamabad. He was involved in the design and development of the engine control computer for a propeller-based UAV engine. After graduation, in 2017, he joined GIK Institute, Pakistan, as an Assistant Professor. He moved to Turkey, in January 2020, as a Postdoctoral Research Associate with Koc University. Recently, he joined the Mechatronics Engineering Department, Istanbul Bilgi University, as an Assistant Professor. His research interests include permanent-magnet linear actuator design for a refrigerator linear compressor, mechatronic system design, system modeling and control, resonance compressors, analog electronics, and instrumentation.

FAISAL KHAN (Member, IEEE) was born in Charsadda, Khyber Pakhtunkhwa, Pakistan, in 1986. He received the B.S. degree in electronics engineering and the M.S. degree in electrical engineering from COMSATS University Islamabad at Abbottabad, Pakistan, in 2009 and 2012, respectively, and the Ph.D. degree in electrical engineering from Universiti Tun Hussein Onn Malaysia, Malaysia, in 2017. From 2010 to 2012, he was a Lecturer with the University of Engineering and Technology, Abbottabad, Pakistan. Since 2017, he has been an Assistant Professor with the Electrical Engineering Department, COMSATS University Islamabad at Abbottabad. He is the author of more than 100 publications, two patents and received multiple research awards. His research interests include design of flux-switching, synchronous, and DC machines. He is a member of the IEEE Industrial Electronics Society and the IEEE-IES Electrical Machines Technical Committee.

NASEER AHMAD was born in Lakki Marwat, Khyber Pakhtunkhwa, Pakistan, in 1992. He received the bachelor's degree in electrical power engineering from the University of Engineering and Technology, Peshawar, in 2015, and the M.S. degree in electrical engineering from COMSATS University Islamabad at Abbottabad, Pakistan, in 2018.

He has been a Lecturer with the Electrical Engineering Department, Balochistan University of Information Technology, Engineering and Management Sciences (BUITEMS), Quetta, Pakistan, since October 2019. His research interests include design and optimization of outer rotor flux switching machine, flux reversal machines, and synchronous machines.

BAKHTIAR KHAN (Member, IEEE) was born in Lower Dir, Khyber Pakhtunkhwa, Pakistan, in 1982. He received the B.Sc. degree in electrical engineering from the University of Engineering and Technology, Peshawar, Pakistan, in 2007, and the M.S. degree in electrical engineering from COMSATS University Islamabad (CUI) at Abbottabad, Pakistan, in 2018, where he is currently pursuing the Ph.D. degree in electrical engineering.

From 2009 to 2014, he worked as a Senior Electrical Engineer with Zahran Group, Saudi Arabia, and from 2015 to 2016, he was the Technical Operation Manager with Seder Group, Saudi Arabia. He is currently a member of the Electric Machine Design Research Group, Department of Electrical and Computer Engineering, CUI at Abbottabad. His research interests include design and analysis of flux switching machines (FSMs) and synchronous machines for high-speed applications.

Mr. Khan is a member of Pakistan Engineering Council.

JONG-SUK RO received the B.S. degree in mechanical engineering from Hanyang University, Seoul, South Korea, in 2001, and the Ph.D. degree in electrical engineering from Seoul National University (SNU), Seoul, in 2008.

He is currently an Associate Professor with the School of Electrical and Electronics Engineering, Chung-Ang University, Seoul. In 2014, he was with the University of Bath, Bath, U.K., as an Academic Visitor. From 2013 to 2016, he worked with the Brain Korea 21 Plus, SNU, as a BK Assistant Professor. He conducted research at the Electrical Energy Conversion System Research Division, Korea Electrical Engineering and Science Research Institute, as a Researcher, in 2013. From 2012 to 2013, he was with the Brain Korea 21 Information Technology, SNU, as a Postdoctoral Fellow. He conducted research at the Research and Development Center, Samsung Electronics, as a Senior Engineer, from 2008 to 2012. His research interests include the analysis and optimal design of intelligent energy conversion systems, such as actuator, generator, and transformer using smart materials, such as electromagnetism, piezoelectric, and shape memory alloy.